Farris *et al. BMC Medical Genomics* (2025) 18:94
https://doi.org/10.1186/s12920-025-02160-1

BMC Medical Genomics

CASE REPORT Open Access

A case of congenital heart defects and familial exudative vitreoretinopathy caused by activation of a cryptic splice donor in *NOTCH1*

Joseph Farris[1], Camila Dergam-Larson[1], Madeline Lopour[2], Kahlen Darr[2], Lisa A. Schimmenti[2], Brittni A. Scruggs[3], Laura J. Lambert[1] and Eric W. Klee[1*]

Abstract

Background *NOTCH1* is associated with two disorders of vascular development, Adams-Oliver Syndrome 5 (AOS5) and aortic valve disease 1 (AOVD1). Here we report a disease-causing variant in *NOTCH1* that has a previously undemonstrated effect on splicing. Additionally, we found that the proband has the optic phenotype of familial exudative vitreoretinopathy (FEVR) which has been reported for probands with pathogenic variants in genes in the notch signaling pathway, but never for *NOTCH1*.

Case presentation The proband presented with a ventricular septal defect, pulmonic stenosis, and ocular findings consistent with familial exudative vitreoretinopathy (FEVR), which *NOTCH1* has not been associated with to date. Trio exome sequencing identified a paternally inherited variant of uncertain significance in *NOTCH1*:c.2153 A > G. We assessed the variant's effect using RT-PCR, finding an increased use of a cryptic donor compared to the control. On this basis, we were able to re-classify this variant as pathogenic.

Conclusions We expand the phenotypic spectrum of *NOTCH1* and contribute to the building evidence that variants in *NOTCH1* cause a spectrum of disorders of vascular development.

Keywords *NOTCH1*, Adams-oliver syndrome, Familial exudative vitreoretinopathy, Rare disease, Splice variant

Introduction

NOTCH1 encodes neurogenic locus Notch homolog protein 1, a receptor protein which broadly regulates cell fate determination. In OMIM, *NOTCH1* is associated with two disorders: Adams-Oliver syndrome type 5 (AOS5; MIM: 616028) and aortic valve disease 1 (AOVD1; MIM: 109730). AOS is a disorder that has historically been defined as the presence of aplasia cutis congenita (ACC), particularly of the scalp, with transverse limb defects. Other features may include congenital heart defects, neurodevelopmental issues, and vision impairment [1]. Stittrich et al. have proposed that the classic ACC and transverse limb phenotypes of Adams-Oliver syndrome are due to vasculopathy caused by *NOTCH1* haploinsufficiency [2].

Variants in *NOTCH1* have also been observed in individuals presenting only cardiac presentation such as various congenital heart defects and no findings of ACC or

*Correspondence:
Eric W. Klee
klee.eric@mayo.edu
[1]Center for Individualized Medicine, Mayo Clinic, Rochester, MN, USA
[2]Department of Clinical Genomics, Mayo Clinic, Rochester, MN, USA
[3]Department of Ophthalmology, Mayo Clinic, Rochester, MN, USA

© The Author(s) 2025. **Open Access** This article is licensed under a Creative Commons Attribution-NonCommercial-NoDerivatives 4.0 International License, which permits any non-commercial use, sharing, distribution and reproduction in any medium or format, as long as you give appropriate credit to the original author(s) and the source, provide a link to the Creative Commons licence, and indicate if you modified the licensed material. You do not have permission under this licence to share adapted material derived from this article or parts of it. The images or other third party material in this article are included in the article's Creative Commons licence, unless indicated otherwise in a credit line to the material. If material is not included in the article's Creative Commons licence and your intended use is not permitted by statutory regulation or exceeds the permitted use, you will need to obtain permission directly from the copyright holder. To view a copy of this licence, visit http://creativecommons.org/licenses/by-nc-nd/4.0/.

limb defects. In 2005, *NOTCH1* was described as the cause of AOVD1 on the basis of two familial variants that segregated with a variety of congenital heart defects along with bicuspid aortic valve and calcification of the aortic valve [3]. A 2019 exome sequencing study found that *NOTCH1* variants were the most frequent cause of non-syndromic tetralogy of Fallot (TOF) [4]. Haploinsufficiency is likely the pathomechanism in *NOTCH1*-related congenital heart defect, as many of these individuals had loss of function (LOF) variants [3, 4], and 2 of 3 tested missense variants associated with TOF showed reduced Notch signaling [4]. Thus, the literature suggests that haploinsufficiency of *NOTCH1* causes a vasculopathy of variable expressivity that may or may not be syndromic.

Methods

Clinical sequencing

Trio exome sequencing was performed by GeneDx (Gaithersburg, PA). Genomic DNA (gDNA) was collected from blood, and coding regions were purified using GeneDx's proprietary capture system. Paired-end reads were sequenced on an NGS platform.

In silico predictions

Missense impact was predicted using REVEL [5]. In silico splicing predictions were made with Splice-AI [6] and visualized using MobiDetails (CHU Montpelier).

RT-PCR

The patient's and a healthy control's RNA sample were purified from white blood cells and used as a template for first-strand cDNA synthesis utilizing Thermo Scientific SuperScriptTM III Reverse Transcriptase and Random Hexamer Primers. The forward primer 5'- A GGGGACCACAGGACCCAACTGC-3', was positioned on Exons 11 and 12, 238 bp upstream of the VUS *NOTCH1*:c.2153A > G, and the reverse primer 5'-GTC TGGCAGTTGGGACCGCTGAA-3', was situated on Exons 14 and 15, 193 bp downstream of the VUS, were utilized to amplify the region of interest within the NOTCH1 gene from the cDNA. The amplification was done using 5x MyTaq Reaction Buffer, MyTaq DNA polymerase, and 5% DMSO with the initial denaturation at 95 °C for 1 min; followed by 35 cycles of denaturation at 95 °C for 15 s, annealing at 58 °C for 15 s, and extension at 72 °C for 5 min. Following this, the PCR product was cloned into a vector utilizing the TOPO™ TA Cloning™ Kit for Sequencing with One Shot™ TOP10 Chemically Competent E. coli. Colonies derived from the cloning process were isolated using the QIAprep® Spin miniprep kit, and the resultant product was sequenced using M13F and M13R primers.

Case & presentation

Presentation

The proband is a four-year-old girl of Indian descent who presented to ophthalmology because of vision impairment due to chorioretinal scarring in her left eye. Testing for infectious causes of scarring, including toxoplasma gondii (repeated three times), toxocara canii (repeated twice) and bartonella, was negative. She had no history of prematurity, being born at a gestational age of 39 weeks 3 days. She had a medical history of moderate to large perimembranous VSD with mild pulmonic stenosis that was repaired at 5 months of age. She was otherwise healthy, and she walked at 9–10 months of age, speaks in full sentences, and is developmentally on target and attending preschool. Her physical examination was notable for no evidence of skin abnormalities, well healed sternal scar, normal digits, and nails. Her family history was concerning with a father who gave a personal history of a self-resolving cardiac septal defect and a paternal uncle who had died in infancy in India from an unspecified heart condition. There was no family history for ophthalmological defects and neither parent was examined (Fig. 1). Her parents are not consanguineous.

Ocular findings

An eye examination under anesthesia was performed. The intraocular pressure, corneal diameters, and anterior chamber were normal in both eyes with no inflammation. Pupils were round with no abnormalities. Refraction confirmed a prescription of + 0.75 sphere right eye and − 6.0 + 2.0 × 090 left eye. On dilated fundus examination, the right eye had several right-angled vessels with subtle straightening of other vessels in the far periphery temporally and nasally that were not visible without scleral depression, but otherwise, the right eye was normal with a healthy appearing optic nerve, fovea, and peripheral retina (Fig. 2A).

The left eye had a large chorioretinal scar throughout the inferior and temporal macula with extension of the scar to the fovea (Fig. 2B &C). This was associated with a small hemorrhage. There was fibrosis on the retinal surface that extended to a prominent temporal ridge. There was a large area of avascular retina 360 degrees mostly affecting the temporal periphery anterior to the ridge (Fig. 2C). The left vasculature was noted to have an abnormal branching pattern in the mid-periphery with right-angled vessels in the periphery (asterisks, Fig. 2B &C). The superior arcade vessel angled sharply inferiorly and extended toward the ridge; the fibrotic hyaloid coursed along this arcade vessel (Fig. 2C). There was a small area of neovascularization along the ridge superiorly. The left optic nerve was tilted and had a larger cup-to-disc ratio (0.6 left vs. 0.3 right) with mild diffuse pallor; there was abnormal vessel insertion to the nerve

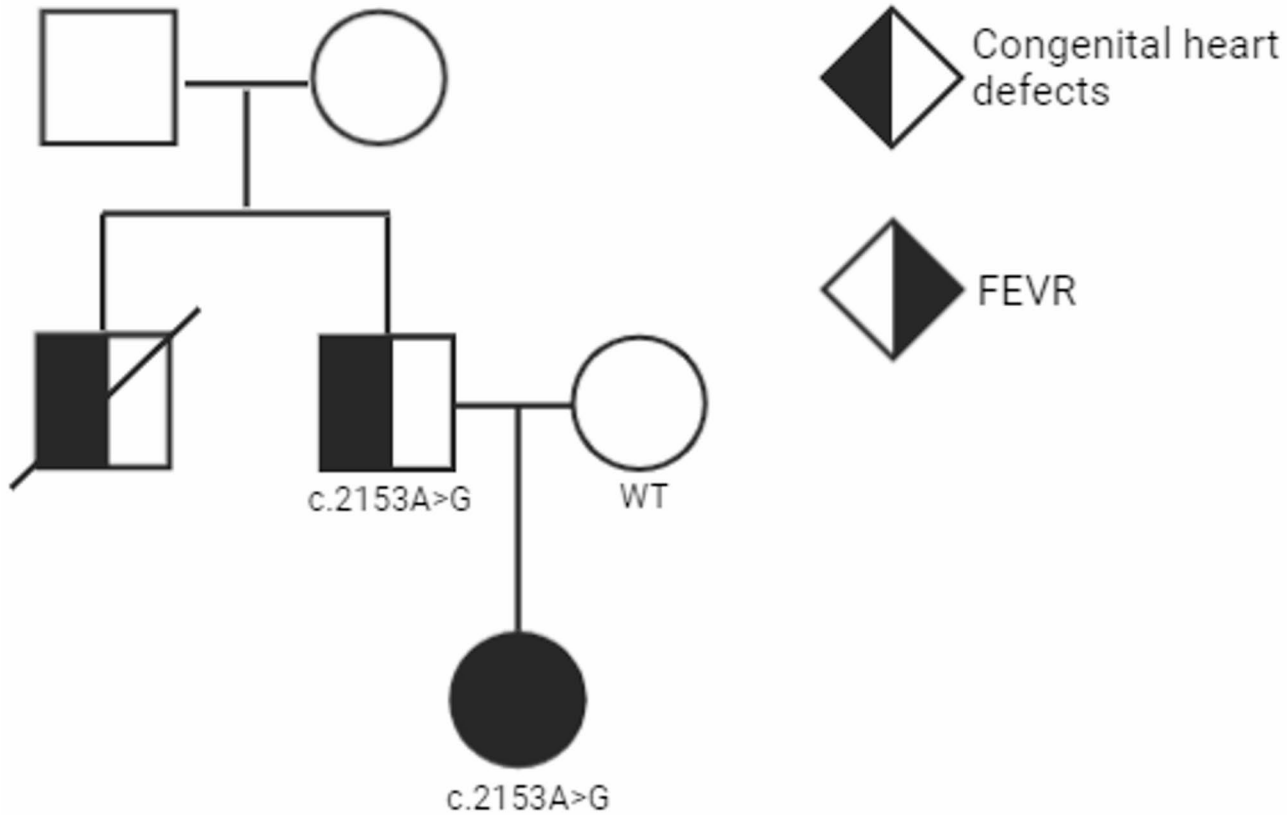

Fig. 1 Pedigree of the proband. The proband had a family history of congenital heart defects with a father self-reporting a self-repairing septal defect. His brother had died in infancy in India of an unspecified heart condition

compared to fellow eye. There was no retinal detachment or significant traction in either eye. The media appeared clear in both eyes.

Fluorescein angiography (RetCam 3; Natus Medical Incorporated, Middleton, WI) was performed. There were subtle vessels changes in the periphery in the right eye, otherwise the right eye appeared normal. There were numerous abnormal coursing vessels noted in the left eye with significant peripheral avascular retina (Fig. 2D) while the right eye appeared grossly normal (Fig. 2E). There was mild leakage in the far periphery superiorly, consistent with the small area of neovascularization along the ridge of the left eye. Optical coherence tomography (Zeiss OPMI Lumera 700, Oberkochen, Germany) was performed in the left eye, confirming the retina had no subretinal fluid or central traction.

The ocular phenotype was most consistent with familial exudative vitreoretinopathy (FEVR), a vision impairment followed with retinal degeneration from the interruption of the blood supply due to abnormal development of blood vessels in the retina, with significant avascular retina, moderate myopia, neovascularization, and prehyaloid hemorrhage. Given the prognosis of increased risk of retinal detachment and vitreous hemorrhage, 1300 argon laser spots were applied to the avascular retina in the left eye to decrease the risk of these neovascularization-related complications.

A vision loss / visual impairment gene panel reported two variants of uncertain significance (VUS's), one in *RP1L1* and the other *PEX26*, both of which are primarily associated with autosomal recessive conditions not consistent with the proband's phenotype. Due to her family history of congenital heart defects and ocular findings, the proband was referred to clinical genomics where she underwent trio exome sequencing.

Exome sequencing

Clinical exome sequencing revealed a paternally-inherited VUS in *NOTCH1*(NM_017617.5):c.2153A > G, which results in the protein change p.(Asn718Ser). The variant is rare, being absent from gnomAD v4.1.0. Missense pathogenicity prediction tool REVEL predicted an uncertain effect with a score of 0.61; however, Splice-AI predicted a significant strengthening of a cryptic donor (score = 0.91) 4 bp upstream of the variant and 59 bp upstream of the canonical exon 13 donor (Fig. 3A). Use of the cryptic donor would result in a frameshift. SpliceVault, a database of splicing events detected in RNA from healthy controls [7], shows that use of this cryptic donor is rare in healthy individuals; it was present in 228 of

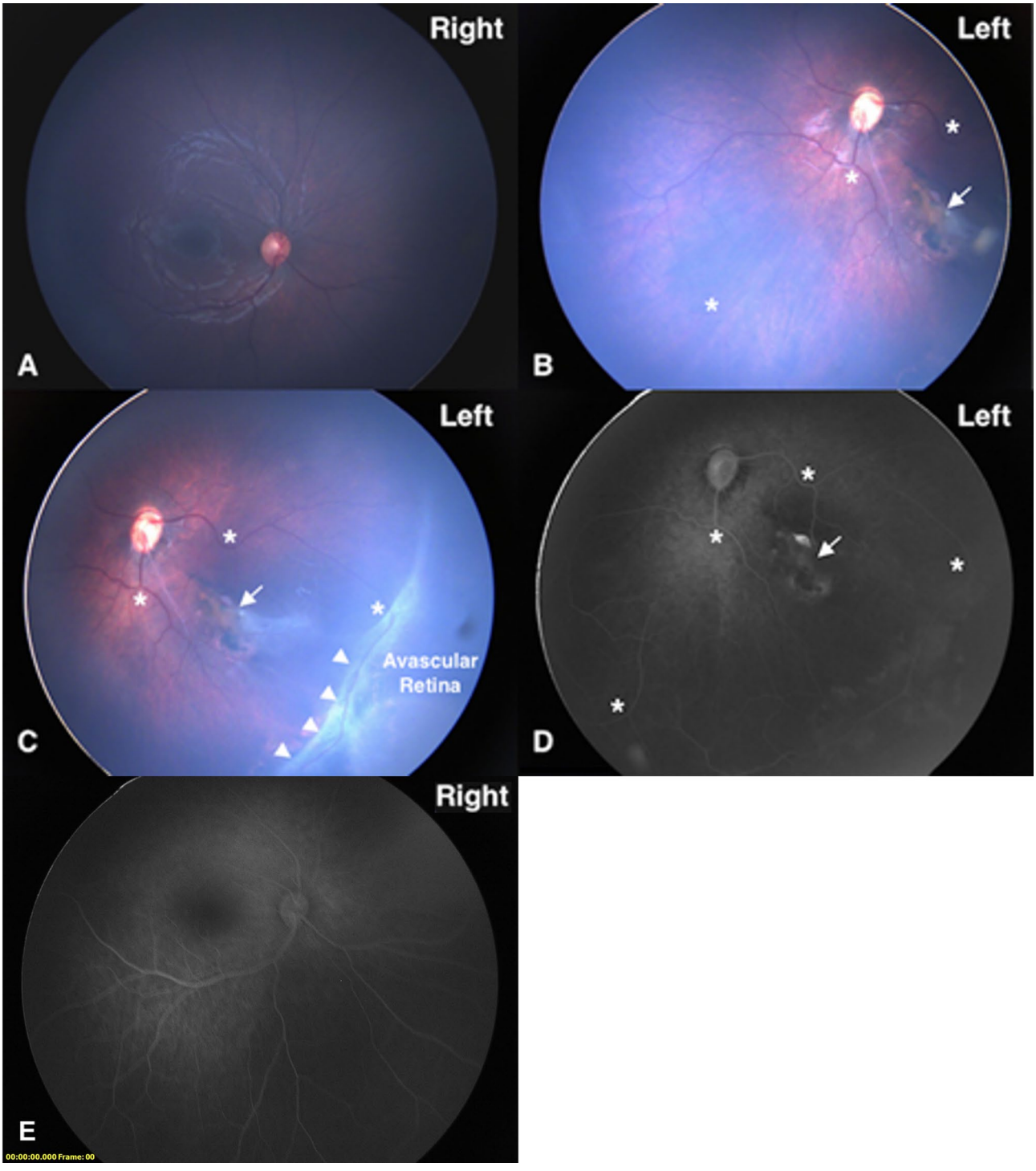

Fig. 2 *NOTCH1*:c.2153 A > G causes an ocular phenotype consistent with familial exudative vitreoretinopathy. (**A**) Color fundus photograph of the right eye shows a normal appearing optic nerve, macula, and posterior pole. (**B-C**) Color fundus photographs of the left eye demonstrate mild pallor of a tilted optic nerve; there are several vessels with abnormal courses (asterisks). There is a chorioretinal scar affecting the fovea (arrow). Fibrosis is seen along a prominent ridge (arrowheads) between the vascular and avascular retina at the equator temporally and inferotemporally. (**D**) Fundus fluorescein angiography of the left eye highlights late staining of the central macular scar (arrow) and the abnormal vasculature (asterisks), including along the temporal ridge. A small area of superior neovascularization is not captured in this image. (**E**) FA of the right is included for comparison

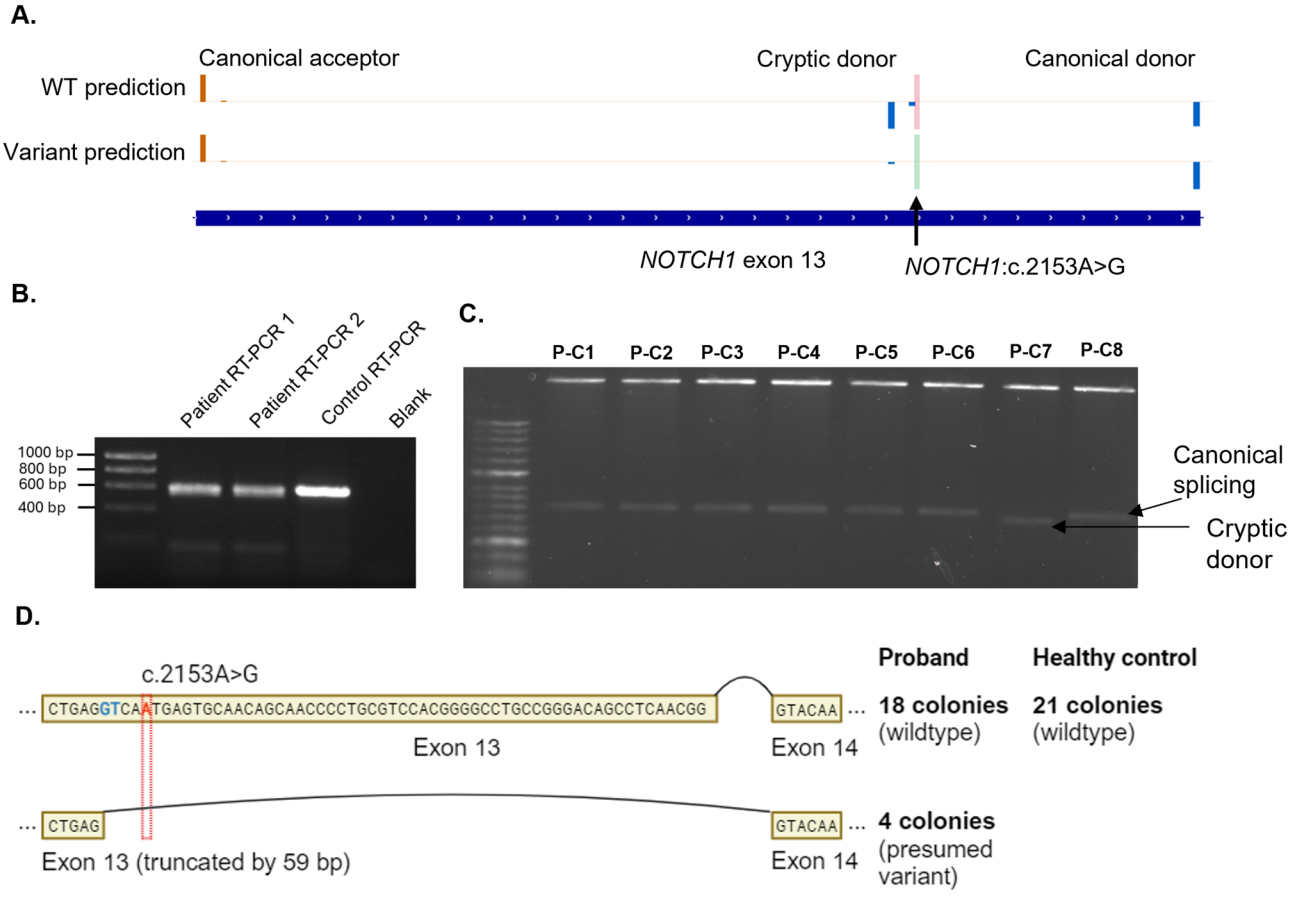

Fig. 3 *NOTCH1*:c.2153A > G causes activation of a cryptic splice donor. (**A**) Splice-AI predictions for *NOTCH1*:c.2153A > G visualized in MobiDetails (CHU Montpelier) [18, 19]. The blue bars represent the strength of a predicted donor. The green highlight represents the wildtype allele, while the red highlight represents the mutant allele. The variant is predicted to cause activation of a cryptic donor 4 bp upstream of the variant with a prediction strength of 0.91 (max score = 1). (**B**) RT-PCR product from the proband (done in duplicate) and a healthy control. (**C**) Eight EcoRI digested plasmids from the proband are included as a reference, with lanes 1–6 and 8 showing canonical splicing, and lane 7 showing the use of the cryptic donor. (**D**) RT-PCR demonstrates allele-specific expression and use of the cryptic donor. A sample wildtype sequence and presumed variant sequence are shown. We cannot definitively say that all use of the frameshifting donor (shown in blue) was due to the variant (position shown in red) because it is used at low levels in the general population. 18 of 22 colonies sequenced (81.8%) showed the wildtype sequence, while 4 (18.2%) showed the presumed variant sequence. The 21 colonies sequenced from the healthy controls all showed canonical splicing. The image was created in BioRender

171,251 control samples (0.1%) with a max read depth of 8 vs. a max read depth of 204 for the canonical donor.

NOTCH1 RT-PCR analysis

Because of the high mis-splicing predictions, the overlap between the congenital heart defects of AOS5 and the proband's phenotype, and the paternal family history, we tested whether the variant causes the predicted splice effect. RT-PCR was performed on RNA collected from the proband's and a control's peripheral blood with primers designed to amplify a 432 bp region encompassing the exon13-exon14 junction in *NOTCH1* (Fig. 3B). The resulting sequences were topo-cloned into a plasmid and transformed into competent *E. coli* colonies. We sequenced 22 colonies and found that 4 of the 22 (18.2%) demonstrated utilization of the cryptic donor connecting to exon 14, while the remaining 18 sequencings (81.8%) were the wildtype allele with canonical splicing (Fig. 3C and D). As mentioned before, the variant c.2153 A > G was downstream the cryptic donor site and therefore was spliced out. Sequencing of 21 colonies from a control all showed the WT sequence. The imbalance between the WT allele and presumed variant allele, 82% vs. 18%, supports the hypothesis of nonsense mediated decay predicted by the resulting frameshift. With the RT-PCR results, we classify this variant as likely pathogenic according to ACMG criteria (Table 1).

Discussion

Here we present the first, to our knowledge, case of a proband with a disease-causing variant in *NOTCH1* and an ocular phenotype that overlaps with FEVR. Many genes currently associated with FEVR are involved in the Norrin/Frizzled4 signaling pathway, including *NDP*,

Table 1 ACMG criteria applied to *NOTCH1*:c.2153 A > G according to ACMG guidelines [17]

Evidence code	Supporting evidence
PVS1	RT-PCR demonstrating allele specific expression and mis-splicing
PM2_supporting	Absent from gnomAD v.4.0
PS4_supporting	Reported in a mother and daughter with congenital heart defects.

FZD4, *LRP5*, and *TSPAN12* [8, 9]. Norrin/Frizzled4 plays an essential role in the development of the retinal vasculature by activating the Wnt signaling pathway [8]. Wnt, in turn, has been shown to upregulate Notch signaling during early vascular development [10]. Notch signaling itself has been shown to play a critical regulatory role in retinal angiogenesis, with endothelial-specific deletion of Notch1 in mice causing an increase in tip cells [11].

The Notch signaling pathway has also been directly implicated in the pathogenesis of FEVR. *JAG1*, which encodes a ligand for NOTCH1, was identified as a candidate gene for FEVR; three FEVR families carried missense variants in *JAG1* that were shown to lead to reduced Notch signaling [12]. Interestingly, FEVR has also been observed in three reported probands with variants in Adams-Oliver genes *DOCK6* [13, 14] and *ARHGAP31* [13]. The individual with the variant in *ARHGAP31* had microcephaly but did not have the classic AOS findings. Thus, while this is the first report of a *NOTCH1* individual with FEVR, the literature supports an association of this ocular phenotype with the Notch signaling pathway and Adams-Oliver syndrome. Adams-Oliver syndrome is also considered a disease with highly variable penetrance and expressivity [15], which may explain the paternal inheritance and rarity of the FEVR phenotype. The description of more probands with pathogenic variants in *NOTCH1* and the FEVR phenotype is necessary to confirm this proposed disease-phenotype association. Given the growing association of the phenotype with genes in the Notch signaling pathway, it is important to report additional cases and consider ophthalmological examination for individuals with pathogenic variants in these genes.

This case demonstrates the importance of considering multiple disease mechanism modalities for functional assay testing. The *NOTCH1* p.(Asn718Ser) variant has previously been reported in a mother with a VSD and her daughter with mitral valve prolapse [16]. The variant was included in a two-variant assay that tested the effect of the variants on Notch signaling and localization. Functional studies demonstrated that p.Asn718Ser was found to have no significant impact compared to the wildtype; however, the experiment was performed using mutant *NOTCH1* cDNA constructs, thus any impact of splicing would not have been observed [16]. Here, we demonstrate with RT-PCR that the variant leads to activation of a cryptic splice donor and consequent loss of function. A limitation of this study is the lack of RNA-seq on patient cells treated with nonsense-mediated decay inhibiting compounds to support our hypothesis that the splice change led to NMD of the affected allele.

Supplementary Information

The online version contains supplementary material available at https://doi.org/10.1186/s12920-025-02160-1.

Supplementary Material 1

Acknowledgements
The authors thank the proband and their family for participating in this study.

Author contributions
JF conceived the study, designed the experiments, analyzed the data, and authored the manuscript. CDL designed and performed the RT-PCR experiments. ML and KD collected clinical data. LAS conceived and oversaw the study and collected clinical data. BAS collected, analyzed, and generated figures for the ophthalmic data. LJL oversaw and designed the RT-PCR experiments and analyzed the data. EWK conceived, oversaw, and provided support for the study. All authors contributed to the authoring and editing of the manuscript.

Funding
This study was supported by the Mayo Clinic Center for Individualized Medicine.

Data availability
Data is provided within the manuscript or supplementary information files.

Declarations

Ethics approval and consent to participate
This study was approved under Mayo Clinic Institutional Review Board #19-003389. Informed consent to participate was obtained from all of the participants in the study. Informed consent to participate was obtained from the parents or legal guardians of any participant under the age of 16. The study adhered to the Declaration of Helsinki.

Consent for publication
Written informed consent for publication of clinical details and/or clinical images was obtained from the parents of the patient.

Competing interests
The authors declare no competing interests.

Received: 18 February 2025 / Accepted: 9 May 2025
Published online: 26 May 2025

References

1. Hassed S, Li S, Mulvihill J, Aston C, Palmer S. Adams-Oliver syndrome review of the literature: refining the diagnostic phenotype. Am J Med Genet A. 2017;173(3):790–800. https://doi.org/10.1002/ajmg.a.37889
2. Stittrich AB, Lehman A, Bodian DL, Ashworth J, Zong Z, Li H, et al. Mutations in NOTCH1 cause Adams-Oliver syndrome. Am J Hum Genet. 2014;95(3):275–84. https://doi.org/10.1016/j.ajhg.2014.07.011

3. Garg V, Muth AN, Ransom JF, Schluterman MK, Barnes R, King IN, et al. Mutations in NOTCH1 cause aortic valve disease. Nature. 2005;437(7056):270–4. https://doi.org/10.1038/nature03940
4. Page DJ, Miossec MJ, Williams SG, Monaghan RM, Fotiou E, Cordell HJ, et al. Whole exome sequencing reveals the major genetic contributors to nonsyndromic tetralogy of fallot. Circ Res. 2019;124(4):553–63. https://doi.org/10.1161/circresaha.118.313250
5. Ioannidis NM, Rothstein JH, Pejaver V, Middha S, McDonnell SK, Baheti S, et al. REVEL: an ensemble method for predicting the pathogenicity of rare missense variants. Am J Hum Genet. 2016;99(4):877–85. https://doi.org/10.1016/j.ajhg.2016.08.016
6. Jaganathan K, Kyriazopoulou Panagiotopoulou S, McRae JF, Darbandi SF, Knowles D, Li YI et al. Predicting Splicing from Primary Sequence with Deep Learning. Cell. 2019;176(3):535–48.e24. https://doi.org/10.1016/j.cell.2018.12.015
7. Dawes R, Bournazos AM, Bryen SJ, Bommireddipalli S, Marchant RG, Joshi H, et al. SpliceVault predicts the precise nature of variant-associated mis-splicing. Nat Genet. 2023;55(2):324–32. https://doi.org/10.1038/s41588-022-01293-8
8. Ye X, Wang Y, Nathans J. The Norrin/Frizzled4 signaling pathway in retinal vascular development and disease. Trends Mol Med. 2010;16(9):417–25. https://doi.org/10.1016/j.molmed.2010.07.003
9. Gilmour DF. Familial exudative vitreoretinopathy and related retinopathies. Eye (Lond). 2015;29(1):1–14. https://doi.org/10.1038/eye.2014.70
10. Corada M, Nyqvist D, Orsenigo F, Caprini A, Giampietro C, Taketo MM, et al. The Wnt/beta-catenin pathway modulates vascular remodeling and specification by upregulating Dll4/Notch signaling. Dev Cell. 2010;18(6):938–49. https://doi.org/10.1016/j.devcel.2010.05.006
11. Hellström M, Phng LK, Hofmann JJ, Wallgard E, Coultas L, Lindblom P, et al. Dll4 signalling through Notch1 regulates formation of tip cells during angiogenesis. Nature. 2007;445(7129):776–80. https://doi.org/10.1038/nature05571
12. Zhang L, Zhang X, Xu H, Huang L, Zhang S, Liu W, et al. Exome sequencing revealed Notch ligand JAG1 as a novel candidate gene for Familial exudative vitreoretinopathy. Genet Med. 2020;22(1):77–84. https://doi.org/10.1038/s41436-019-0571-5
13. Tao Z, Bu S, Lu F. Two AOS genes attributed to Familial exudative vitreoretinopathy with microcephaly: two case reports. Med (Baltim). 2021;100(9):e24633. https://doi.org/10.1097/md.0000000000024633
14. Jin EZ, Huang LZ, Zhao MW, Yin H. Atypical Adams-Oliver syndrome with typical ocular signs of Familial exudative vitreoretinopathy. Int J Ophthalmol. 2022;15(8):1249–53. https://doi.org/10.18240/ijo.2022.08.04
15. Kutlubay Z, Pehlivan Ö. Adams-Oliver syndrome. Int J Dermatol. 2014;53(3):352–4. https://doi.org/10.1111/j.1365-4632.2012.05533.x
16. Chapman G, Moreau JLM, Szot IPE, Iyer JO, Shi KR. Functional genomics and gene-environment interaction highlight the complexity of congenital heart disease caused by Notch pathway variants. Hum Mol Genet. 2020;29(4):566–79. https://doi.org/10.1093/hmg/ddz270
17. Richards S, Aziz N, Bale S, Bick D, Das S, Gastier-Foster J, et al. Standards and guidelines for the interpretation of sequence variants: a joint consensus recommendation of the American college of medical genetics and genomics and the association for molecular pathology. Genet Med. 2015;17(5):405–24. https://doi.org/10.1038/gim.2015.30
18. Baux D, Van Goethem C, Ardouin O, Guignard T, Bergougnoux A, Koenig M, et al. MobiDetails: online DNA variants interpretation. Eur J Hum Genet. 2021;29(2):356–60. https://doi.org/10.1038/s41431-020-00755-z
19. de Sainte Agathe JM, Filser M, Isidor B, Besnard T, Gueguen P, Perrin A, et al. SpliceAI-visual: a free online tool to improve spliceai splicing variant interpretation. Hum Genomics. 2023;17(1):7. https://doi.org/10.1186/s40246-023-00451-1

Publisher's note

Springer Nature remains neutral with regard to jurisdictional claims in published maps and institutional affiliations.